applied sciences

MDPI

Article

Upcycling Alum Sludge as a Reinforcement in PBAT Composites: A Sustainable Approach to Waste Valorisation

Dongyang Sun [1], Thomas Henthorn [1], Carmen-Mihaela Popescu [2] and Reza Salehiyan [1,*]

[1] School of Computing, Engineering and Built Environment, Edinburgh Napier University, 10 Colinton Road, Edinburgh EH10 5DT, UK; d.sun@napier.ac.uk (D.S.); 40498975@live.napier.ac.uk (T.H.)

[2] Petru-Poni Institute of Macromolecular Chemistry of the Romanian Academy, 41A Grigore Ghica Voda Alley, RO700487 Iasi, Romania; mihapop@icmpp.ro

* Correspondence: r.salehiyan@napier.ac.uk

Abstract: This study explores the valorisation of alum sludge, a byproduct of water treatment processes, as a sustainable reinforcement material in Poly(butylene adipate-co-terephthalate) (PBAT) composites. The research aims to address industrial waste challenges by developing eco-friendly composite materials while promoting circular economy principles. Alum sludge particles, classified into two size distributions (<63 µm and <250 µm), were incorporated into PBAT matrices at varying concentrations. The composites were characterised for their mechanical, thermal, crystallographic, and moisture adsorption properties; and their biodegradation behaviour was evaluated through soil burial tests over 60 days. The results revealed that the 63 µm particle size fraction exhibited superior performance compared to the 250 µm fraction, demonstrating improved mechanical properties, reduced degradation rates, and enhanced interfacial bonding. Composites with 5 wt.% alum sludge achieved a balance between reinforcement and processability, outperforming the other filler concentrations examined. This innovative approach highlights the potential of upcycling alum sludge into functional materials, advancing sustainable waste management and composite manufacturing. Furthermore, the observed variation in degradation rates suggests that these composites can be tailored for applications requiring controlled compostability.

Keywords: waste valorisation; sustainable composites; alum sludge; PBAT; biodegradable

Academic Editors: Francisco Jesús Fernández Morales, Jose Luis García-Morales and Miguel Suffo

Received: 31 January 2025
Revised: 22 February 2025
Accepted: 25 February 2025
Published: 27 February 2025

Citation: Sun, D.; Henthorn, T.; Popescu, C.-M.; Salehiyan, R. Upcycling Alum Sludge as a Reinforcement in PBAT Composites: A Sustainable Approach to Waste Valorisation. *Appl. Sci.* **2025**, *15*, 2591. https://doi.org/10.3390/app15052591

1. Introduction

The rapid expansion of the global population and industrialisation has significantly increased waste generation across domestic, agricultural, and industrial sectors [1]. These unwanted byproducts of human activity pose severe challenges to environmental sustainability. Domestic waste is a major contributor, with approximately 2 billion tonnes of municipal solid waste generated annually, a figure projected to rise to 2.59 billion tonnes by 2030 [2]. Agricultural waste, which includes residues from crop production (e.g., straw and husks), livestock activities (e.g., manure and bedding materials), and agro-industrial processes (e.g., fruit peels and bagasse), also contributes substantially to the global waste stream [3]. In less developed regions, a significant portion of agricultural waste is treated through open burning due to limited access to advanced waste management technologies, leading to environmental pollution and health risks [4]. Additionally, industrial waste, including byproducts from manufacturing, mining, and chemical processes, contributes another 20 million tonnes of hazardous and non-hazardous waste to ecosystems annually [5,6]. Research has increasingly focused on innovative waste management strategies, particularly for industrial waste. For instance, Fang et al. developed a whole-cell biocatalyst capable of effectively depolymerising polyethylene terephthalate (PET) plastic from industrial waste [7], while Lu et al. investigated the upcycling of fly ash from incineration processes into green binders via flue-gas-enhanced wet carbonation [8]. Other studies have explored the use of lime sludge as a filler in polymer matrix composites, suggesting a sustainable technique that improves commercial viability and reduces manufacturing costs [9].

Amongst the various types of industrial wastes, alum sludge has drawn significant attention due to its environmental impact. Alum sludge is a byproduct of water treatment processes employing aluminium-based coagulants, such as aluminium sulphate (alum), to remove impurities. During treatment, alum reacts with water to form aluminium hydroxide, which aggregates suspended particles into larger flocs. These flocs settle as sludge, consisting primarily of aluminium hydroxide, organic matter, and other insoluble impurities, with up to 5% water by volume. The disposal of alum sludge is a persistent challenge for water treatment plants, with landfilling remaining the most common practice. However, increasing environmental regulations and public awareness have driven efforts to explore sustainable alternatives. Studies have investigated the reuse of alum sludge as an adsorbent [10], a component in building bricks [11], and a cementitious material [12]. Additional research has examined its potential applications in agriculture, for example, as a soil conditioner [13] or a substrate in constructed wetlands [14]. Despite these advancements, limited research has explored the use of alum sludge as a functional filler in polymer matrix composites, leaving a gap for further exploration in this area.

Polymer matrix composites (PMCs) have become increasingly important due to their unique combination of lightweight, high-strength, and versatile properties. While polyolefin-based plastics are commonly used as matrix materials, there is growing demand for more environmentally friendly polymers, such as Poly(butylene adipate-co-terephthalate) (PBAT). PBAT is a biodegradable aliphatic–aromatic copolyester that offers high flexibility, excellent processability, and biodegradability, making it an ideal candidate for sustainable composite materials [15,16]. PBAT has gained more attention in recent years for use in PMC manufacturing, thanks to its promising properties (e.g., high elongation at break) and environmental benefits (e.g., ability to break down naturally). To enhance the mechanical, thermal, and barrier properties, fibres or particles are incorporated with the polymer as reinforcements. For instance, natural fibres such as jute [17] and hemp [18] have been combined with PBAT to produce biodegradable composites suitable for packaging and other engineering applications. Additionally, nanoscale particles like cellulose nanocrystals [19] and titania nanoparticles [20] have been integrated into PBAT matrices to optimise processability and improve thermal and mechanical properties.

A recent study has shown that PBAT can be combined with agricultural waste, such as rice husks [21] and wheat straw [22], presenting a sustainable solution for waste valorisation while reducing the environmental impact through the use of biodegradable polymers. These innovations demonstrate the potential of PBAT-based composites as a solution for sustainable composite manufacturing while contributing to a circular economy. Inspired by this, the team identified a research gap regarding incorporating alum sludge into PBAT composites to establish a novel industrial waste valorisation strategy. The aim of the work was to investigate the feasibility of using alum sludge as a functional filler in biodegradable composite manufacturing, converting undervalued industrial waste into useful products.

The work firstly examined how alum sludge particle size influences the mechanical properties and biodegradation behaviour of the composites. Smaller particle sizes are reported to provide larger surface areas per unit volume, enabling more uniform stress transfer, which is critical for improving both mechanical properties and biodegradation performance [23]. Additionally, research suggests that a polydisperse mixture of particles can significantly affect the elastic modulus [24], highlighting the potential of optimised size distributions in enhancing composite performance. In this study, the alum sludge was pre-treated and categorised into two size distributions before being incorporated into PBAT to form composite samples. These composites were characterised for their mechanical properties and biodegradation behaviours; the latter were assessed through a composting test, in which the composites were buried in soil for 60 days. This methodological approach not only evaluates degradation over time but also provides insights into the lifecycle performance of biodegradable materials. The results highlight the role of alum sludge, in different size distributions, in influencing both the degradation rate and mechanical performance, aiding in the optimisation of composite formulations for improved environmental sustainability.

Moreover, composite samples with varying alum sludge concentrations were also prepared and characterised to evaluate how the loading of sludge particles affects composites' mechanical, thermal, and crystallographic properties, as well as their moisture adsorption behaviour. The findings contribute to the development of an innovative composite material that incorporates valorised waste materials, offering enhanced functionality and economic viability. By demonstrating a sustainable approach to utilising industrial byproducts in composite manufacturing, this work addresses key challenges in material sustainability and underscores the broader potential of waste-derived materials in high-performance applications.

2. Materials and Methods

2.1. Materials

Poly(butylene adipate-co-terphthalate) (PBAT), marketed under the trade name of Ecoflex F Blend C1200 (BASF, Ludwigshafen, Germany), was used as the polymer matrix in this study. It has a density of 1.25–1.27 g/cm^3, a tensile strength of 35–44 MPa, and an elongation of 560–710%, as reported in the Supplier's Material datasheet and supported by relevant publications [25]. Alum sludge was sourced from Scottish Water of the Rosebery Water Treatment Works in Midlothian, Scotland.

2.2. Alum Sludge Pre-Treatment and Alum Sludge/PBAT Composite Preparation

Figure 1 illustrates the complete process for the pre-treatment of alum sludge and the preparation of composite samples using PBAT. The alum sludge was collected from the water treatment plant in the form of a dewatered cake (Figure 1a). It was firstly oven-dried at 110 °C for 24 h to remove excess moisture and improve processability. The oven-dried sludge, which formed small crumbs (Figure 1b), was then subjected to ball milling in roller bottles containing zirconia balls (Orto Alresa Roller Mill), operating at 10 rpm for four hours. The milled material was then sieved using a shaker stack to obtain distinct size fractions: particles smaller than 63 µm (denoted as 63 µm particles; Figure 1c) and particles smaller than 250 µm (denoted as 250 µm particles; Figure 1d). The images highlight the differences in particle size distributions between these two alum sludge fractions. Additional SEM observations, presented in the Supplementary document, reveal that the sludge particles exhibit irregular shapes, heterogeneous surfaces, and a porous texture. These morphological characteristics are consistent with findings reported elsewhere [26]. The two sets of sludge samples were stored in airtight containers to maintain their properties for subsequent composite processing.

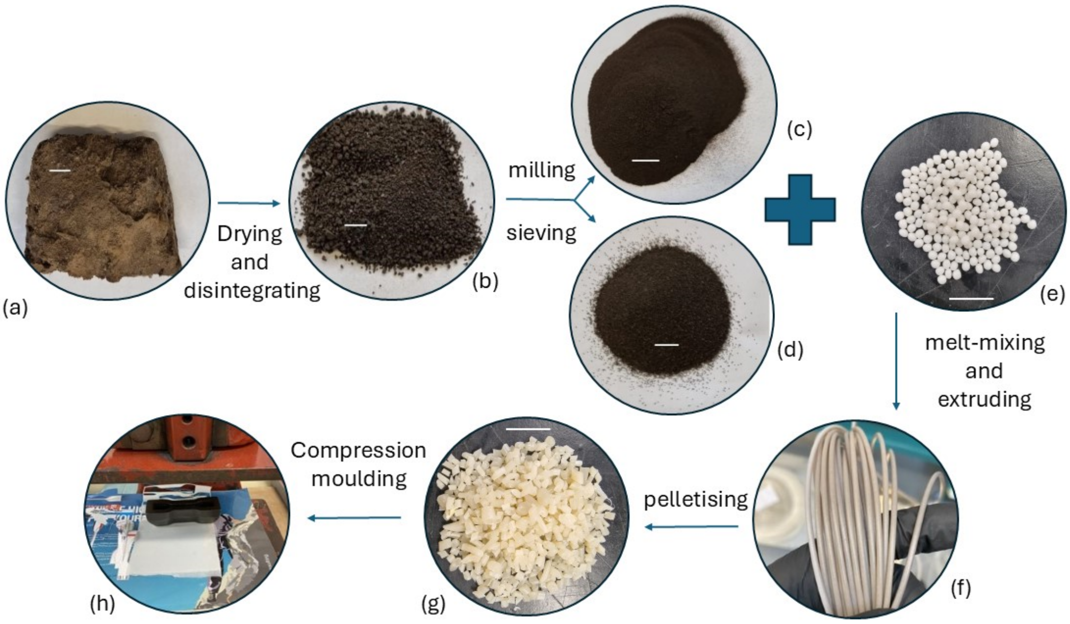

Figure 1. Overview of the alum sludge pre-treatment and composite preparation process; the scale bar corresponds to 10 mm. The process includes (**a**) dewatered alum sludge cake, (**b**) oven-dried alum sludge crumbs, (**c**) fine alum sludge fraction (<63 µm), (**d**) coarser alum sludge fraction (<250 µm), (**e**) PBAT pellets, (**f**) extruded filaments for composite processing, (**g**) composite pellets obtained after pelletising, and (**h**) compression-molded composite sheets.

PBAT pellets were dried in an oven at 110 °C for four hours to remove any absorbed moisture (Figure 1e). Approximately 200g of PBAT polymer was used to prepare both neat and composite samples. A single-screw melt extruder (Davis Standard BC-32) was operated at an outlet temperature of 150 °C and a screw speed of 8 rpm to process the material, producing filaments (Figure 1f) using various formulations. The extruded filaments were pelletised using a Rieter Primo 50 pelletiser. The resulting pellets (Figure 1g) were then compression-moulded at 160 °C to form 1 mm thick sheets, which were subsequently shaped into dogbone specimens for mechanical testing (Figure 1h).

For the composite sample preparation, alum sludge particles (63 µm and 250 µm particle fractions) were incorporated into the PBAT matrix at a filler concentration of 5 wt.%. These composite samples underwent mechanical testing and soil burial testing to evaluate the influence of particle size distribution on composite performance. Based on the results, additional composite samples were prepared using the 63 µm fraction sludge, with filler concentrations of 2 wt.%, 10 wt.%, and 20 wt.%, to further investigate the effect of filler concentration on composite properties.

2.3. Soil Burial Test

A composting study was conducted to evaluate the degradation of neat PBAT and PBAT composites containing 5 wt.% alum sludge particles (63 µm and 250 µm) under real soil burial conditions. The testing procedure was designed in accordance with ASTM D5988-12 and ISO 14855 and a previously reported work [27]. Vegetable compost was used as the burial medium. Five dogbone-shaped specimens were prepared for each composite type, along with an additional specimen for weight loss measurements. The specimens were buried vertically at an average depth of 8 cm. The burial tests were performed in a controlled-environment chamber, maintaining a constant temperature of approximately 30 °C and a relative humidity of about 83.9%, measured using a particle counter (PCE Instruments, Manchester, UK). The initial weights of all specimens were recorded using a digital scale. Subsequent measurements were taken at 15-day intervals. At each interval, the specimens were carefully retrieved, cleaned, and oven-dried at 60 °C for four hours before mechanical testing and weight loss assessments.

2.4. Mechanical Testing

The mechanical properties of the alum sludge/PBAT composites and neat PBAT were examined. The tensile strength, Young's modulus, and % elongation at break of the samples were measured using a universal testing machine (Z030; ZwickRoell, Ltd., Worcester, UK) with a 5 kN load cell and a crosshead speed of 5 mm/min, following the ASTM D638 guidelines. Dogbone-shaped specimens were cut from 1 mm sheets, and five replicates were tested for each formulation to calculate average values and standard deviations. The results are reported as mean values with standard deviations to reflect measurement variability.

2.5. Differential Scanning Calorimetry (DSC)

The thermal properties of the alum sludge/PBAT composites and neat PBAT were evaluated using a differential scanning calorimeter (PerkinElmer 8000; Perkin Elmer UK, Buckinghamshire, UK). Approximately 10 mg of each sample was weighted and sealed in stainless steel pans. The samples were analysed over a temperature range of −5 °C to 200 °C at a rate of 10 °C/min under a constant nitrogen gas purge (20 mL/min) to maintain an inert atmosphere and minimise oxidation.

The analysis included two heating cycles. During the first cycle, the samples were heated to 200 °C to eliminate any thermal history and then cooled to −5 °C. In the second cycle, the samples were reheated to 200 °C to observe structural changes, such as crystallisation, melting transitions, or any rearrangement in the composite material. Key thermal parameters, including crystallisation temperature (T_c), melting temperature (T_m), and associated enthalpy changes, were extracted from the resulting thermograms.

2.6. X-Ray Diffraction

The X-ray diffraction (XRD) patterns were obtained using a Bruker D8 Advance diffractometer (Germany) equipped with Cu-Kα radiation (λ = 0.1542 nm), a parallel beam with a Gobel mirror, and a dynamic scintillation detector. The instrument operated at an accelerating voltage of 40 kV and a current of 30 mA. Data were collected over a scanning range of 5° to 40° (2θ).

2.7. Determination of Dynamic Water-Vapour Sorption Behaviour

The dynamic water-vapour sorption behaviour of the composite samples was analysed using a dynamic vapour sorption (DVS) apparatus (DVS Intrinsic; Surface Measurement Systems Ltd., London, UK). Measurements were conducted at three relative humidity (RH) levels: 65%, 75%, and 85%, under room-temperature conditions. Each test began with an initial drying step at 0% RH to remove residual moisture, followed by exposure to the target RH level until the sample mass stabilised (defined as a change of less than 0.002% over a 10 min period). Time vs. mass change curves were generated for the PBAT composites containing 5 wt.%, 10 wt.%, and 20 wt.% alum sludge and compared with the neat PBAT.

3. Results and Discussion

3.1. Analysis of Biodegradation During Composting

Two composite samples incorporating alum sludge fractions of 63 µm and 250 µm were compared with the neat PBAT for their biodegradation performance. The tensile strength, % elongation at break, Young's modulus, and weight loss of the composite samples at different compositing stages (0 day, 15 days, 30 days, and 60 days) are presented in Figure 2. Over the 60-day compositing period, a progressive decline in tensile strength and % elongation at break was observed for all samples (Figure 2a,b). The composite with the 250 µm particle fraction exhibited the greatest reduction at the end of 60 days, with decreases of 55.16% and 63.59% in tensile strength and % elongation at break, respectively, compared to the undegraded samples. In contrast, the composite with the 63 µm particle fraction experienced a sharp reduction in tensile strength and % elongation at break by 15 days (−32.66% and −33.66%) but demonstrated greater resistance to degradation thereafter. Values recorded at 30 and 45 days showed pronounced variability, as indicated by the larger error bars in the graph.

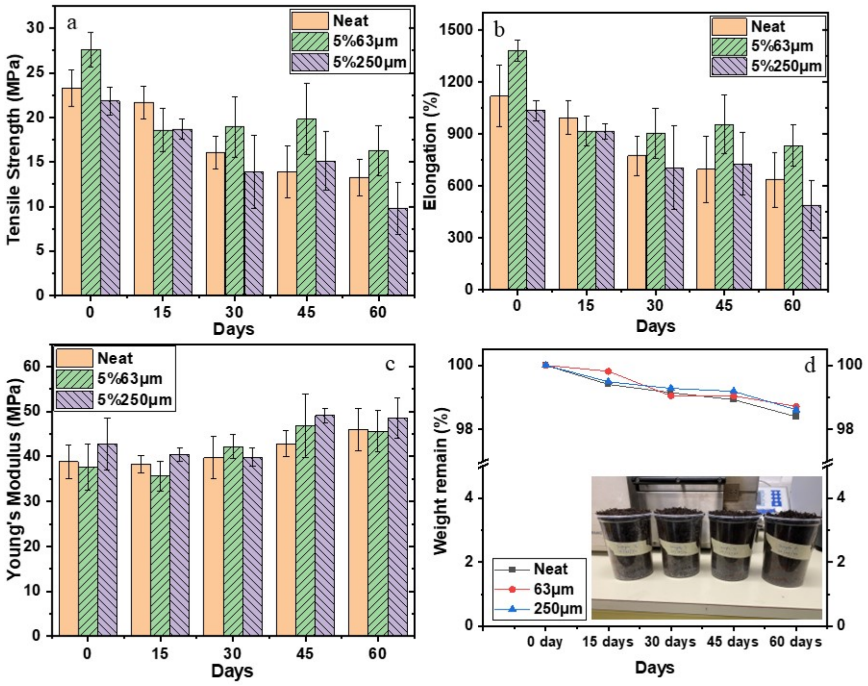

Figure 2. Composting analysis of the alum sludge/PBAT composites and neat PBAT, including (**a**) tensile strength, (**b**) % elongation at break, (**c**) Young's modulus, and (**d**) weight loss over a 60-day composting period. The insert in (**d**) shows sample preparation for composting using vegetable composts.

Regarding Young's modulus (Figure 2c), a slight increasing trend in stiffness was observed for all samples up to 45 days, after which the rate of change became less significant. This trend can be attributed to the preferential degradation of the amorphous regions in the polymer during composting, which increases crystallinity and, consequently, stiffness. A similar observation was reported by Xu et al., where the crystallinity of the PBAT polymer was increased after enzymatic degradation [27]. Once the amorphous regions are largely degraded, the rate of degradation slows, requiring a longer period for further breakdown. This explains the plateau observed in the Young's modulus vs. composting days curve.

Figure 2d indicates the weight loss of all samples throughout the composting period. The neat PBAT sample exhibited the highest weight loss of 1.6% at 60 days, while the 63 µm sample showed the least weight loss, indicating its higher resistance to degradation. This observation aligns with the result in the tensile strength analysis and accelerated UV degradation tests (data are provided in the Supplementary document). The 63 µm sample exhibited a sharp reduction in weight within the first 15 days, followed by a slower rate of degradation. This trend suggests a two-stage degradation mechanism: an initial rapid degradation phase followed by a slower degradation phase. The initial phase (the rapid degradation stage) was driven by microorganisms breaking down the more accessible regions of the sample, such as the surface or the amorphous regions of the polymer. In contrast, the subsequent phase (the slow degradation stage) was limited by reduced microbial penetration and diffusion into the less accessible regions, such as the inner parts of the sample or the crystalline regions of the polymer. The improved resistance to degradation observed in the 63 µm sample, as reflected in its better-maintained mechanical properties and reduced weight loss, could be attributed to the higher surface area of the smaller particles, which facilitates stronger interfacial bonding between the alum sludge and the PBAT matrix. This finding suggests that such waste particles can be used to prepare composites for applications requiring extended compostability, allowing for the fine-tuning of degradation rates to match specific timeframes.

Figure 3a illustrates the stress–strain curves for the samples after 60 days of composting. Notably, small irregularities ("bumps") appear in the stress profiles of the degraded samples, which are absent in their respective control samples that did not undergo any degradation (i.e., neat PBAT, 63 µm, and 250 µm samples at 0 day; their graph is provided in the Supplementary document). This phenomenon is likely due to microtear formation during sample stretching, caused by the activity of hydrophilic microorganisms within the alum sludge filler. These microorganisms may create a more porous polymer matrix, making it more susceptible to localised tearing. The visual inspections of the samples after 30 and 60 days, as shown in Figure 3b,c, revealed progressive darkening and surface deterioration, particularly in the 250 µm sample. This evidence aligns with the mechanical property trends observed earlier, where the 250 µm sample exhibited greater degradation compared to the 63 µm sample.

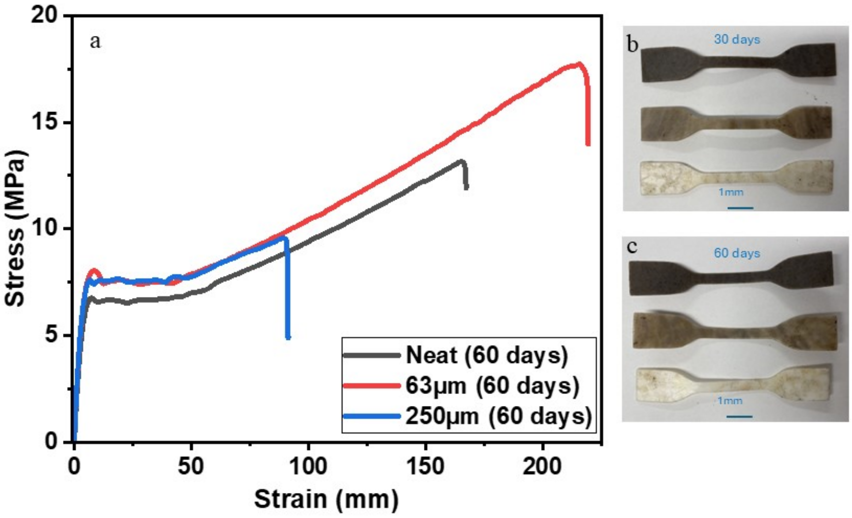

Figure 3. (**a**) Stress vs. strain curves of degraded samples of neat PBAT, 63 µm composite, and 250 µm composite and (**b**,**c**) their visual inspection (samples from bottom to top: neat PBAT, 63 µm composite, and 250 µm composite).

Overall, the results indicate that the 63 µm composite outperforms the 250 µm composite in all evaluated aspects. As a result, the alum sludge with the 63 µm particle size fraction was selected for further investigation into the effect of filler concentration on the mechanical, thermal, and moisture adsorption properties of the composite, as discussed in the subsequent sections.

3.2. Mechanical Properties

The effects of alum sludge addition on the mechanical properties of the composites are presented in Figure 4. The tensile strength results (Figure 4a) indicate that the 2 wt.%

composite sample exhibits a value comparable to neat PBAT, albeit with a relatively large error bar. A marginal increase in tensile strength can be observed for the 5 wt.% sample, while a significant reduction occurs at higher filler concentrations (10 wt.% and 20 wt.%). This trend suggests a balance between the reinforcing effect of the filler and the adverse effects caused by processing challenges.

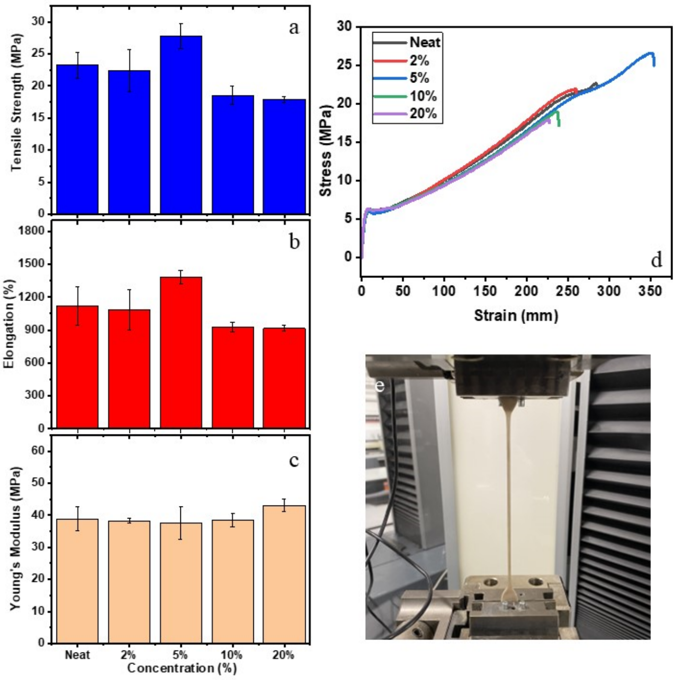

Figure 4. Mechanical properties of neat PBAT and its composites with alum sludge at various concentrations: (**a**) tensile strength, (**b**) % elongation at break, (**c**) Young's modulus, (**d**) representative stress vs. strain curves, and (**e**) an image showing elongation of the 5 wt.% composite sample during tensile testing.

It is well recognised that particles incorporated into composite materials may act as barriers to stress and crack propagation when they are well-dispersed, enhancing a material's resistance to mechanical deformation and improving its overall strength [28]. In this study, such reinforcement effects were more pronounced in samples with lower filler concentrations. The processing method employed appeared to facilitate better particle dispersion, consistent interfacial bonding, and minimal disruption to the PBAT matrix at 2 wt.% and 5 wt.% filler levels, resulting in an effective reinforcement mechanism. This was particularly evident in the 5 wt.% sample. In contrast, at higher filler concentrations, poor particle dispersion and agglomeration became dominant, leading to detrimental effects. Numerous studies, such as those by Cosmoiu et al. [29], Fu et al. [30], and Mostovoy et al. [31], have analysed how agglomeration creates localised stress points that reduce the mechanical strength of composite materials. Similarly, in this study, the agglomerated regions of alum sludge particles in the polymer matrix serve as stress concentration sites, hindering effective load transfer and disrupting matrix continuity. This reduces the composite's overall strength and increases its susceptibility to brittle fracture.

The % elongation at break of the composite samples was generally lower than that of neat PBAT (Figure 4b), as the addition of particles restricts the matrix's plastic deformation, resulting in a stiffer and less ductile material. Similar trends have been widely reported in the literature [32]. Interestingly, the 5 wt.% sample showed an anomalous increase in % elongation at break (Figure 4e), which could be attributed to an optimised filler concentration that promotes improved dispersion and interfacial bonding of the composite phases. However, further investigation is needed to confirm this hypothesis. Additionally, the significant error bars observed for many samples emphasise the need to test a larger number of specimens to ensure statistical reliability.

Figure 4c shows the Young's moduli for the PBAT polymer and the composites. A gradual increase in modulus with a higher filler concentration can be observed, indicating enhanced rigidity due to the reinforcement particles restricting plastic deformation in the matrix. However, this reinforcement effect is relatively modest, which is possibly attributed to the amorphous nature of alum sludge. Previous studies [33] have shown that non-heat-treated, dried alum sludge exhibits low crystallinity, which limits its contribution to modulus enhancement compared to crystalline fillers. Figure 4d depicts the tensile behaviour of the studied samples: a linear elastic region before the yield point, followed by plastic deformation for all samples.

3.3. Thermal Behaviour Analysis

Differential Scanning Calorimetry (DSC) analysis was conducted to determine the thermal parameters of the samples, including T_m (melting temperature), T_c (crystallisation temperature), ΔH_m (melting enthalpy), and ΔH_c (crystallisation enthalpy). These values were extracted from the DSC cooling and second heating thermograms of the neat PBAT polymer and alum sludge/PBAT composites with various alum sludge concentrations, as illustrated in Figures 5a and 5b, respectively, and are summarised in Table 1. The degree of crystallinity was calculated using Equation (1).

$$X_c(\%) = \frac{\Delta H_m}{1 - \alpha \times \Delta H_{m0}} \times 100 \tag{1}$$

where ΔH_{m0} is the crystallisation enthalpy of 100% PBAT, taken as 114 J/g [34], and α is the alum sludge content in the composite.

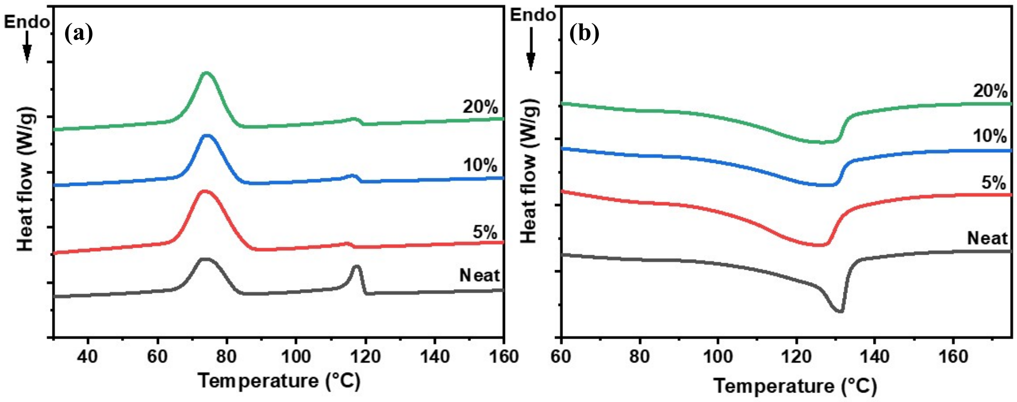

Figure 5. DSC analysis of (**a**) crystallisation exotherms during the first cooling cycle and (**b**) melting endotherms during the second heating cycle for neat PBAT and alum sludge/PBAT composites.

Table 1. DSC analysis for thermal properties of alum sludge/PBAT composites.

Sample	T_c (°C)	ΔH_c (J/g)	T_m (°C)	ΔH_m (J/g)	X_c (%)
Neat	74.58	11.11	129.15	18.51	16.24
5 wt.%	74.38	14.44	121.92	15.49	14.30
10 wt.%	74.68	12.12	121.61	13.77	13.42
20 wt.%	74.43	11.94	119.56	13.85	15.19

The incorporation of alum sludge into the PBAT matrix resulted in a reduction in the melting temperature of the composites, with the decrease becoming progressively more pronounced as the sludge concentration increased. For instance, the 20 wt.% sludge sample exhibited a T_m reduction of approximately 20% compared to the neat PBAT polymer. A similar trend was observed for the melting enthalpy and degree of crystallinity, both of which decreased as the filler concentration increased. These reductions could be attributed to the disruption of the crystalline structure in the PBAT matrix. Since alum sludge is amorphous and has a low crystallinity, its distribution in the PBAT matrix decreases the amount of polymer available to form crystalline regions, thereby lowering the melting temperature. Secondly, the presence of sludge may interfere with polymer chain alignment, further reducing the extent of crystallinity and the thermal energy required for melting.

Figure 5 shows the crystallisation exotherms and melting endotherms for all samples. In Figure 5a, the crystallisation exotherms become broader as the alum sludge concentration increases. This broadening suggests that the sludge, with its low molecular mobility, acts as a physical battier, hindering the crystallisation of PBAT and slowing the rate of crystallisation [35]. The small peaks (119~120 °C) and big peaks (~74 °C) could be attributed to the crystalline regions of the butylene adipate (BA) and the crystalline phase of poly butylene terephthalate, respectively [36,37]. The melting endotherms in Figure 5b become progressively broader with increasing alum sludge concentrations. In contrast, composites with lower sludge concentrations exhibit a sharper rise in heat flow after the melting peak (T_m), closely resembling the behaviour of neat PBAT. This suggests that higher filler concentrations may impede the flow of the molten composite, likely due to sludge particles disrupting polymer chain mobility. It is important to note that DSC analysis is highly sensitive to measurement uncertainties, particularly due to factors such as baseline drift, instrument calibration, and small sample sizes. Minor variations in sample mass and potential contamination can influence heat flow measurements, which may introduce slight discrepancies in the reported values. While the DSC results in this study provide insights into the relative thermal behaviours of the composites, they may not fully capture the bulk properties of the composite materials.

3.4. X-Ray Diffraction (XRD) Analysis

The diffractograms of neat PBAT, alum sludge, and their composites with varying concentrations of alum sludge are presented in Figure 6. The neat PBAT sample exhibits distinct diffraction peaks at 16.3°, 17.4°, 20.3°, 21.6°, 23.2°, and 24.8° 2θ, corresponding to (011), (010), (110), (100), and (111) crystalline diffraction planes [38], respectively. These peaks are superimposed on a broad amorphous background, confirming the semicrystalline nature of PBAT. In contrast, the alum sludge sample does not display any diffraction peaks, indicating its amorphous or low-crystallinity nature, which is consistent with observations from previous studies.

The incorporation of alum sludge into the PBAT matrix does not shift the positions of the diffraction peaks, indicating that the crystalline structure of PBAT remains unaffected by the addition of alum sludge. However, as the concentration of sludge increases in the composites, a noticeable reduction in peak intensity can be observed. This decrease suggests a reduction in the overall crystallinity of the composite materials, which mirrors the observations from the DSC analysis. The decline in crystallinity can be attributed to the disruption of the polymer chain arrangements, as discussed in the previous section. Since alum sludge is amorphous, it likely hinders the ordered packing of PBAT chains, thereby reducing the crystalline regions within the composite matrix.

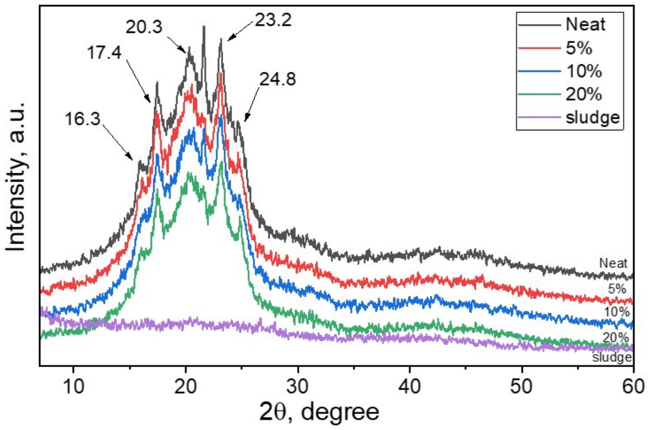

Figure 6. XRD patterns of neat PBAT, alum sludge, and alum sludge/PBAT composites containing 5 wt.%, 10 wt.%, and 20 wt.% alum sludge.

3.5. Dynamic Vapour Sorption Analysis

Dynamic vapour sorption (DVS) analysis was conducted to compare the moisture sorption behaviour of the PBAT composites with varying alum sludge contents to that of neat PBAT. All samples were initially de-moisturised at 0% RH before being exposed to RH levels of 65%, 75%, and 85% at room temperature. The % mass change as a function of time is shown in Figure 7.

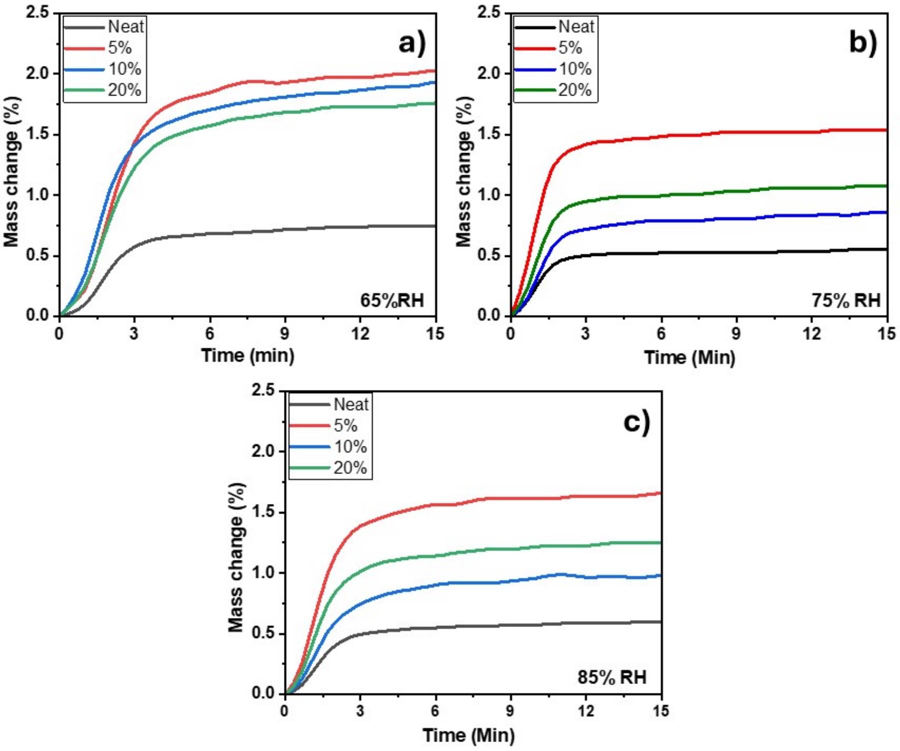

Figure 7. Dynamic vapour sorption curves of alum sludge PBAT composites with 0 wt.%, 5 wt.%, 10 wt.%, and 20 wt.% weight percent at (**a**) 65% RH, (**b**) 75% RH, and (**c**) 85% RH at room temperature.

At all RH levels, the composites exhibit distinct sorption kinetics compared to neat PBAT. During the initial uptake stage, the composites demonstrate significantly faster sorption rates, as evidenced by the steeper slopes of the sorption curves. These increased rates are attributed to the hydrophilic nature of alum sludge, which enhances moisture diffusion pathways within the composite. The hydroxyl-rich surfaces and porous structure of alum sludge readily interact with water molecules, facilitating rapid sorption, as highlighted by Awab et al. and Zhao et al. [39,40].

However, no clear correlation was observed between alum sludge concentration and sorption rate across the RH levels. At 65% RH, the slopes for the 5 wt.%, 10 wt.%, and 20 wt.% composites are comparable, with the 10 wt.% sample exhibiting slightly higher sorption after approximately 1 min. At 75% and 85% RH, the 5 wt.% composite demonstrates the fastest sorption rate, suggesting that higher alum sludge concentrations may lead to particle aggregation, obstructing effective moisture diffusion pathways. All samples approach saturation within 6 min at 65% RH and within 3 min at 75% and 85% RH.

In terms of maximum moisture gain (MMG), all composite samples absorb more moisture than the neat PBAT, indicating a reduction in hydrophobicity due to the addition of alum sludge. Alum sludge is assumed to enhance water adsorption in composites through its hydroxyl-rich surface and porous structure, suggesting a proportional relationship between alum sludge content and MMG in alum sludge composite materials. However, the results revealed that the 5 wt.% composite achieved the highest MMG, followed by the 20 wt.% and 10 wt.% composites. This disparity implies that 5 wt.% alum sludge enables optimal particle dispersion within the polymer matrix, whereas higher concentrations promote aggregation, reducing the effective surface area for water interaction.

4. Conclusions

This study bridges the fields of waste management and sustainable composite materials by developing and characterising PBAT composites reinforced with alum sludge. The findings reveal that alum sludge incorporation influences the mechanical, thermal, and environmental properties of the composite, with the 63 μm fraction exhibiting superior performance among the two tested particle size distributions. Additionally, the concentration of alum sludge in the PBAT matrix significantly influenced mechanical properties and moisture adsorption behaviours, with higher concentrations leading to agglomeration and processability challenges. Furthermore, the presence of alum sludge was found to affect the biodegradation behaviour, thermal behaviour, and crystallinity of the composites, all of which are critical factors for the material to be used in the real-world application. This work introduces an innovative approach to alum sludge valorisation, offering an alternative solution to its direct landfill disposal. The team acknowledge that alum sludge contains aluminium-derived compounds, which may limit its use in applications involving direct human contact or exposure to aquatic environments. However, this study highlights its potential for sustainable manufacturing, particularly in construction materials or infrastructure for water treatment facilities, where exposure risks can be effectively managed. By transforming industrial waste into functional composite materials, this research contributes to a balanced strategy that promotes both waste upcycling and broader environmental sustainability in responsible waste management.

Supplementary Materials: The following supporting information can be downloaded at: https://www.mdpi.com/article/10.3390/app15052591/s1.

Author Contributions: Conceptualisation, D.S. and R.S.; methodology, D.S., T.H., C.-M.P. and R.S.; formal analysis, T.H.; writing-original draft preparation, D.S.; writing-review and editing, D.S., T.H., C.-M.P. and R.S. All authors have read and agreed to the published version of the manuscript.

Funding: This research was partially funded by the International Collaboration Fund, funded by the Scottish Government, Scottish Funding Council, and facilitated by Research Innovation Scotland.

Institutional Review Board Statement: Not applicable.

Informed Consent Statement: Not applicable.

Data Availability Statement: The data supporting the results in this study are provided in the Supplementary document included with this submission, which contains the data for the figures.

Acknowledgments: The authors gratefully acknowledge the support provided by Edinburgh Napier University and Research Innovation Scotland.

Conflicts of Interest: The authors declare no conflict of interest.

References

1. Lu, M.; Zhou, C.; Wang, C.; Jackson, R.B.; Kempes, C.P. Worldwide scaling of waste generation in urban systems. *Nat. Cities* **2024**, *1*, 126–135. [CrossRef]
2. Maalouf, A.; Mavropoulos, A.; El-Fadel, M. Global municipal solid waste infrastructure: Delivery and forecast of uncontrolled disposal. *Waste Manag. Res.* **2020**, *38*, 1028–1036. [CrossRef]
3. Xu, Q.; Zhang, T.; Niu, Y.; Mukherjee, S.; Abou-Elwafa, S.F.; Nguyen, N.S.H.; Al Aboud, N.M.; Wang, Y.; Pu, M.; Zhang, Y.; et al. A comprehensive review on agricultural waste utilization through sustainable conversion techniques, with a focus on the additives effect on the fate of phosphorus and toxic elements during composting process. *Sci. Total Environ.* **2024**, *942*, 173567. [CrossRef] [PubMed]
4. Bhuvaneshwari, S.; Hettiarachchi, H.; Meegoda, J.N. Crop residue burning in India: Policy challenges and potential solutions. *Int. J. Environ. Res. Public Health* **2019**, *16*, 832. [CrossRef] [PubMed]
5. Mesjasz-Lech, A. Trends of Industrial Waste Generation in Manufacturing Enterprises in the Context of Waste Prevention—Shift-Share Analysis for European Union Countries. *Sustainability* **2025**, *17*, 34. [CrossRef]
6. Chen, J.; Zeng, B.; Xu, W.; Hu, S.; Wang, S.; Wang, K.; Zhang, W.; Wu, S.; Song, Z. Mechanical behaviour and damage constitutive model of semi-circular arch tunnels with straight walls under soaking conditions. *Eng. Fail. Anal.* **2025**, *169*, 109137. [CrossRef]
7. Fang, Y.; Chao, K.; He, J.; Wang, Z.; Chen, Z. High-efficiency depolymerization/degradation of polyethylene terephthalate plastic by a whole-cell biocatalyst. *3 Biotech* **2023**, *13*, 138. [CrossRef]
8. Lu, M.; Ge, W.; Xia, Y.; Sun, C.; Lin, X.; Tsang, D.C.; Ling, T.-C.; Hu, Y.; Wang, L.; Yan, J. Upcycling MSWI fly ash into green binders via flue gas-enhanced wet carbonation. *J. Clean. Prod.* **2024**, *440*, 141013. [CrossRef]
9. Kashyap, S.; Datta, D. Reusing industrial lime sludge waste as a filler in polymeric composites. *Mater. Today Proc.* **2017**, *4 Pt A*, 2946–2955. [CrossRef]
10. Djekoune, L.; Maaliou, A.; Salem, Z.; Ziani, D.; Kamel, R.; Ouakouak, A.; Baigenzhenov, O.; Bokov, D.O.; Ivanets, A.; Hosseini-Bandegharaei, A. Phosphate adsorption on dried alum sludge: Modeling and application to treatment of dairy effluents. *Environ. Res.* **2024**, *252*, 118976. [CrossRef]
11. Ewais, E.M.M.; Elsaadany, R.M.; Ahmed, A.A.; Shalaby, N.H.; Al-Anadouli, B.E.H. Insulating Refractory Bricks from Water Treatment Sludge and Rice Husk Ash. *Refract. Ind. Ceram.* **2017**, *58*, 136–144. [CrossRef]
12. Ahmed, F.R.; Muhammad, M.A.; Ibrahim, R.K. Effect of alum sludge on concrete strength and two way shear capacity of flat slabs. *Structures* **2022**, *40*, 991–1001. [CrossRef]
13. Kluczka, J.; Zołotajkin, M.; Ciba, J.; Staroń, M. Assessment of aluminum bioavailability in alum sludge for agricultural utilization. *Environ. Monit. Assess.* **2017**, *189*, 422. [CrossRef] [PubMed]
14. Zhao, X.; Zhao, Y.; Wang, W.; Yang, Y.; Babatunde, A.; Hu, Y.; Kumar, L. Key issues to consider when using alum sludge as substrate in constructed wetland. *Water Sci. Technol.* **2015**, *71*, 1775–1782. [CrossRef]
15. Siegenthaler, K.O.; Künkel, A.; Skupin, G.; Yamamoto, M. Ecoflex® and Ecovio®: Biodegradable, Performance-Enabling Plastics. In *Synthetic Biodegradable Polymers*; Rieger, B., Künkel, A., Coates, G., Reichardt, R., Dinjus, E., Zevaco, T., Eds.; Springer: Berlin/Heidelberg, Germany, 2012; pp. 91–136.
16. Martín-Poyo, C.; Cerisuelo-Ferriols, J.P.; Badia-Valiente, J.D. Influence of Vinyl Acetate-Based and Epoxy-Based Compatibilizers on the Design of TPS/PBAT and TPS/PBAT/PBSA Films. *Appl. Sci.* **2025**, *15*, 456. [CrossRef]
17. Sudha, G.S.; Aswathy, N.R.; Biswal, M.C.; Mohapatra, A.K. Investigating the reinforcing effect of jute fiber in a PLA & PBAT biopolymer blend matrix for advanced engineering applications: Enhancing sustainability with bioresources. *Mater. Today Commun.* **2024**, *40*, 109960.
18. Lamsaf, H.; Singh, S.; Pereira, J.; Poças, F. Multifunctional properties of PBAT with hemp (*Cannabis sativa*) micronised fibres for food packaging: Cast films and coated paper. *Coatings* **2023**, *13*, 1195. [CrossRef]
19. Pinheiro, I.F.; Ferreira, F.V.; De Holanda Saboya Souza, D.; Gouveia, R.F.; Lona, L.M.F.; Morales, A.R.; Mei, L.H.I. Mechanical, rheological and degradation properties of PBAT nanocomposites reinforced by functionalized cellulose nanocrystals. *Eur. Polym. J.* **2017**, *97*, 356–365. [CrossRef]
20. Venkatesan, R.; Rajeswari, N. TiO_2 nanoparticles/poly(butylene adipate-co-terephthalate) bionanocomposite films for packaging applications. *Polym. Adv. Technol.* **2017**, *28*, 1699–1706. [CrossRef]

21. Wang, L.; Wang, Z.; Peng, L.; Wang, L.; Deng, B. Degradation Behavior of Rice Husk Fiber-Reinforced PLA/PBAT Composites in Short-Term Hydrothermal Environment. *J. Appl. Polym. Sci.* **2025**, *142*, e56646. [CrossRef]
22. Feng, J.; Zhang, W.; Wang, L.; He, C. Performance comparison of four kinds of straw/PLA/PBAT wood plastic composites. *BioResources* **2020**, *15*, 2596. [CrossRef]
23. Alaei, M.H.; Mahajan, P.; Brieu, M.; Kondo, D.; Rizvi, S.J.A.; Kumar, S.; Bhatnagar, N. Effect of particle size on thermomechanical properties of particulate polymer composite. *Iran. Polym. J.* **2013**, *22*, 853–863. [CrossRef]
24. Semeykina, V.; Appiah, C.; Rothberg, S.; Heinrich, S.; Giuntini, D.; Schneider, G.A. Expectations vs. reality in nacre-like composites: Dominating role of particle packing and polymer confinement in mechanical performance. *Adv. Compos. Hybrid Mater.* **2024**, *8*, 65. [CrossRef]
25. Siegenthaler, K.O.; Künkel, A.; Skupin, G.; Yamamoto, M. Ecoflex® and Ecovio®: Biodegradable, Performance-Enabling Plastics. In *Synthetic Biodegradable and Biobased Polymers: Industrial Aspects and Technical Products*; Künkel, A., Battagliarin, G., Winnacker, M., Rieger, B., Coates, G., Eds.; Springer International Publishing: Cham, Switzerland, 2024; pp. 111–175.
26. Thabet, R.; Fouad, M.K.; El Sherbiny, S.A.; Tony, M.A. Zero-Waste Approach: Assessment of Aluminum-Based Waste as a Photocatalyst for Industrial Wastewater Treatment Ecology. *Int. J. Environ. Res.* **2022**, *16*, 36. [CrossRef]
27. Xu, J.; Feng, K.; Li, Y.; Xie, J.; Wang, Y.; Zhang, Z.; Hu, Q. Enhanced Biodegradation Rate of Poly(butylene adipate-co-terephthalate) Composites Using Reed Fiber. *Polymers* **2024**, *16*, 411. [CrossRef]
28. Meng, Q.; Wang, T. An improved crack-bridging model for rigid particle-polymer composites. *Eng. Fract. Mech.* **2019**, *211*, 291–302. [CrossRef]
29. Cosmoiu, I.; Apostol, D.A.; Picu, C.R.; Constantinescu, D.M.; Sandu, M.; Sorohan, S. Influence of Filler Dispersion on the Mechanical Properties of Nanocomposites. *Mater. Today Proc.* **2016**, *3*, 953–958. [CrossRef]
30. Fu, S.-Y.; Feng, X.-Q.; Lauke, B.; Mai, Y.-W. Effects of particle size, particle/matrix interface adhesion and particle loading on mechanical properties of particulate–polymer composites. *Compos. Part B Eng.* **2008**, *39*, 933–961. [CrossRef]
31. Mostovoy, A.; Bekeshev, A.; Tastanova, L.; Akhmetova, M.; Bredihin, P.; Kadykova, Y. The effect of dispersed filler on mechanical and physicochemical properties of polymer composites. *Polym. Polym. Compos.* **2020**, *29*, 583–590. [CrossRef]
32. Shi, Q.; Cui, P.; Hu, M.; Wang, F.; Xu, H.; Zhou, X. Solid-State Synthesis of SiC Particle-Reinforced AZ91D Composites: Microstructure and Reinforcement Mechanisms. *Metals* **2024**, *14*, 434. [CrossRef]
33. Sun, D.; Saw, B.L.H.; Onyianta, A.J.; Wang, B.; Wilson, C.; O'rourke, D.; See, C.H.; Popescu, C.-M.; Dorris, M.; Shyha, I.; et al. Preparation of elastomeric nanocomposites using nanocellulose and recycled alum sludge for flexible dielectric materials. *J. Adv. Dielectr.* **2023**, *13*, 2242008. [CrossRef]
34. Chivrac, F.; Kadlecová, Z.; Pollet, E.; Avérous, L. Aromatic Copolyester-based Nano-biocomposites: Elaboration, Structural Characterization and Properties. *J. Polym. Environ.* **2006**, *14*, 393–401. [CrossRef]
35. Li, M.; Jia, Y.; Shen, X.; Shen, T.; Tan, Z.; Zhuang, W.; Zhao, G.; Zhu, C.; Ying, H. Investigation into lignin modified PBAT/thermoplastic starch composites: Thermal, mechanical, rheological and water absorption properties. *Ind. Crops Prod.* **2021**, *171*, 113916. [CrossRef]
36. Salehiyan, R.; Kim, M.C.; Xia, T.; Jin, S.; Nofar, M.; Chalmers, L.; Hyun, K. Enhanced re-processability of poly (butylene adipate-co-terephthalate) (PBAT) via chain extension toward a more sustainable end-of-life. *Polym. Eng. Sci.* **2024**, 1–13. [CrossRef]
37. Pietrosanto, A.; Scarfato, P.; Di Maio, L.; Nobile, M.R.; Incarnato, L. Evaluation of the Suitability of Poly(Lactide)/Poly(Butylene-Adipate-co-Terephthalate) Blown Films for Chilled and Frozen Food Packaging Applications. *Polymers* **2020**, *12*, 804. [CrossRef]
38. Meng, D.; Xie, J.; Waterhouse, G.I.N.; Zhang, K.; Zhao, Q.; Wang, S.; Qiu, S.; Chen, K.; Li, J.; Ma, C.; et al. Biodegradable Poly(butylene adipate-co-terephthalate) composites reinforced with bio-based nanochitin: Preparation, enhanced mechanical and thermal properties. *J. Appl. Polym. Sci.* **2020**, *137*, 48485. [CrossRef]
39. Awab, H.; Paramalinggam, P.T.; Yusoff, A.R.M. Characterization of alum sludge for reuse and disposal. *Malays. J. Fundam. Appl. Sci.* **2012**, *8*, 209–213. [CrossRef]
40. Zhao, W.; Xie, H.; Li, J.; Zhang, L.; Zhao, Y. Application of Alum Sludge in Wastewater Treatment Processes: "Science" of Reuse and Reclamation Pathways. *Processes* **2021**, *9*, 612. [CrossRef]